South Polar Layered Deposits of Mars: The cratering record

Michelle Koutnik, Shane Byrne, and Bruce Murray
Geological and Planetary Science, California Institute of Technology, Pasadena, California, USA

Received 18 October 2001; revised 30 January 2002; accepted 16 July 2002; published 8 November 2002.

[1] Data from the Mars Orbiter Laser Altimeter (MOLA) and Mars Orbiter Camera (MOC) instruments aboard the Mars Global Surveyor (MGS) were used in a detailed search of a selected part of the South Polar Layered Deposits (SPLD) for impact craters. Impact craters with diameters from 0.8 to 5 km were identified from a MOLA-derived shaded relief map and were primarily validated using individual MOLA tracks and, in select cases, MOC narrow angle images. The resultant crater population determined in this study is at least four times the density of the crater population previously recognized. From these new statistics, we estimate the mean apparent surface age of the SPLD to be 30–100 Ma, depending on the established production model isochrons used. All of these craters are considerably shallower than other Martian craters in the same diameter range. We attribute this shallowness to be the cause of the lower detection rates of previous studies. There is a correlation between crater depth and rim height, which suggests that both erosion and infilling have affected the crater forms. A similar study of the north polar layered deposits uncovered no craters in this diameter range. A limited population of craters smaller than 800 m was uncovered in higher-resolution MOC narrow angle images. These do not appear to have been degraded to the same degree. This separate population implies a surface exposure age of only 100,000 years and perhaps indicates an event that erased all small craters and degraded and infilled the larger ones. *INDEX TERMS:* 5420 Planetology: Solid Surface Planets: Impact phenomena (includes cratering); 5462 Planetology: Solid Surface Planets: Polar regions; 5470 Planetology: Solid Surface Planets: Surface materials and properties; 6225 Planetology: Solar System Objects: Mars

Citation: Koutnik, M., S. Byrne, and B. Murray, South Polar Layered Deposits of Mars: The cratering record, *J. Geophys. Res.*, *107*(E11), 5100, doi:10.1029/2001JE001805, 2002.

1. Introduction

[2] The Martian Polar Layered Deposits (PLD) are believed to provide critical insight into recent Martian climatic changes [*Murray et al.*, 1972; *Cutts et al.*, 1976; *Howard et al.*, 1982; *Plaut et al.*, 1988; *Thomas et al.*, 1992]. The surface age determined for the PLD has been used as a reference age for polar processes and as a key factor in constraining the global climate history of Mars. To better estimate the age of the South Polar Layered Deposits (SPLD) we have conducted a Mars Global Surveyor (MGS) based search for impact craters using a Mars Orbiter Laser Altimeter (MOLA) shaded relief map, profiles of individual MOLA tracks, and Mars Orbiter Camera (MOC) images. This search has resulted in identification of at least four times the density of impact craters on the SPLD than previously recognized [*Plaut et al.*, 1988] using Viking imagery data. The craters observed and included in this study are argued to have originated as primary impacts on the uppermost surface of the SPLD. There has likely been a complicated history of burial, erosion, and perhaps exhumation of individual craters on the SPLD that cannot be discerned precisely from this data. Hence, the resulting crater population provides an "apparent surface age", which is a measure of how long this unit has been exposed at the surface. We have found that our impact crater population is unevenly distributed across the sample study area of the SPLD. The term "mean apparent surface age" is used here because different portions of the sample study area of the SPLD do not appear to be the same age based on this distribution.

[3] The cratering record for the PLD was previously estimated from analysis of Viking Orbiter images and from selected Mariner 9 images [*Cutts et al.*, 1976; *Plaut et al.*, 1988; *Herkenhoff and Plaut*, 2000]. These images are of limited completeness for crater recognition due to seasonal frost, atmospheric obscuration, and effective image resolution. The annual seasonal frost deposition and sublimation cycle cause variations in surface albedo, especially in spring and in some summer images when the frost cover is nonuniform though still present. Atmospheric haze, particularly as found in the north polar region [*Kahn*, 1984], can cause significant surface obscuration. The effective surface resolution of Viking images limited the size and degree of modification of impact craters that could be confidently identified. Using Viking imagery, *Plaut et al.* [1988] were able to identify 15 "likely" impact craters and 7 "possible" impact craters greater than 800 m in diameter over 1.1×10^6

0148-0227/02/2001JE001805$09.00

km^2, approximately 80% of the entire exposed SPLD. Initially, *Plaut et al.* [1988] assigned a surface age of approximately 120 Ma but the cratering flux used in this estimate was reconsidered by *Herkenhoff and Plaut* [2000] to be very low and a new surface age was estimated. Using the *Plaut et al.* [1988] data, model estimates by *Herkenhoff and Plaut* [2000] assigned an SPLD surface age of 14.5 ± 7.2 Ma using a "nominal" cratering rate (two times the lunar value, R(20) = 5.6) or 7.25 ± 3.6 Ma using a "high" cratering rate (four times the lunar value, R(20) = 11.2), where R(D) is the number of craters with diameters greater than D produced on an area of 1×10^6 km^2 in 1 billion years.

[4] The MOLA and MOC instruments aboard the MGS have been returning extensive data of the entire planet [*Albee et al.*, 2001], with especially complete coverage near the poles. Due to the amount of near polar coverage high resolution MOLA shaded relief maps can be made. The MOLA shaded relief map exposes remarkable surficial detail that is generally better than that seen in visible images of comparable nominal resolution (i.e., Viking Orbiter images, MOC wide-angle (WA) images). This is due to the freedom from clouds, haze, surface frost, and especially due to the high proportion of returned laser energy from within each ~100 m footprint of the MOLA instrument [*Zuber et al.*, 1992]. When compared to an optical imaging system, MOLA exhibits an unusually high modulation transfer function. The MOLA instrument can resolve slopes of 1 part in 1000 on any length scale that is greater than about 330 meters [*Neumann et al.*, 2001]. Precisely colocated topography data from the MOLA instrument and in select cases high-resolution imagery from the MOC have provided the new data for the detailed study of impact craters on the SPLD reported here.

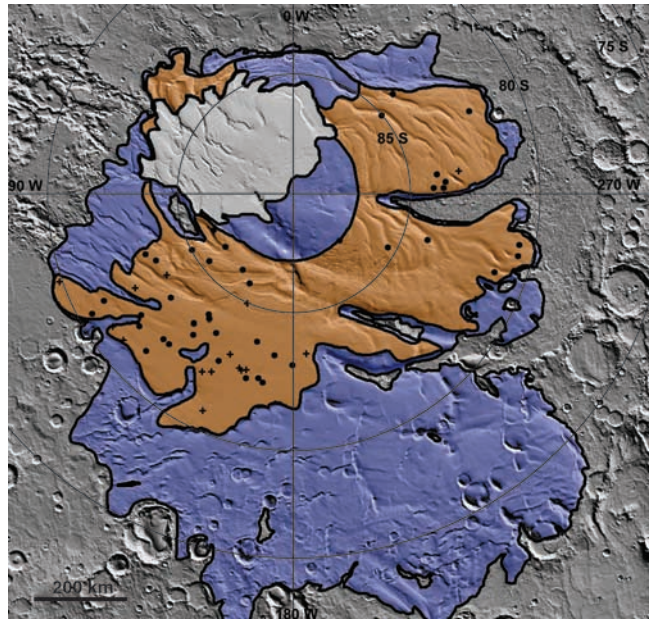

Figure 1. MOLA shaded relief map covering the SPLD. The sample area, shaded orange contains all the impact craters examined in this study. The regions shaded blue cover the most inclusive boundary of the mapped SPLD [*Kolb and Tanaka*, 2001] and have been excluded. The likely crater locations are marked by a "●" and the possible crater locations are marked by a "+." The white shaded region is the approximate outline of the residual cap, also excluded in the sample study area. Only two craters in the study area were previously recognized as "likely" by *Plaut et al.* [1988].

2. Data Sources and Methodology

2.1. Data Sources

[5] We have made MOLA shaded relief maps following the method of *Nuemann et al.* [2001], using MOLA data through June 2000. The shaded relief map used in our study has been projected into polar stereographic coordinates and exhibits a resolution of approximately 200 m/pixel. The shaded relief map showing the boundary of the SPLD [*Kolb and Tanaka*, 2001], including our study area with marked crater locations, is shown in Figure 1. The choice of study area is described in section 2.2.

[6] All circular, negative features identified from the MOLA shaded relief map were initially considered to be potential impact craters. Due to the MOLA map resolution a choice of approximately 800 m was made as our limiting feature diameter. Most crater measurements were done on individual MOLA tracks or on the MOLA shaded relief map and, when applicable, MOC data sets displayed in the commercial Environmental Systems Research Institute (ESRI) product Geographical Information Systems (GIS) ArcView developed at Caltech for Mars polar use.

[7] As the next step to validate the potential impact craters identified from the MOLA shaded relief map, the individual MOLA tracks within a 1.5 km diameter circle of all the potential craters included in this study were collected and the best crossing tracks were chosen. From these individual tracks the features identified from the MOLA shaded relief map were confirmed or rejected as impact craters. Many of the negative features in the MOLA shaded relief map turned out to be artifacts, not real surface features, generally resulting from single MOLA point error in individual MOLA tracks used to make the shaded relief map.

[8] Crater diameter was measured from the MOLA shaded relief map because this data set incorporates all the data and is higher resolution than individual MOLA tracks. A measure of crater depth and rim height was made from the crossing MOLA track showing the most relief. The measure of crater depth is likely an underestimate of the true value because the crossing MOLA tracks did not necessarily align with the centers of the impact craters.

[9] We define a "likely" and a "possible" impact crater population that is defined in detail in section 2.3 and is consistent with the classification of *Plaut et al.* [1988]. We found a population of 36 likely impact craters and 12 possible impact craters. Figure 2 shows one of the MOLA tracks used to validate each crater in the population of 36 likely impact craters and 12 possible impact craters in the 0.8–5 km diameter range. The chosen tracks shown exemplify the MOLA tracks used in all cases of validation as an impact crater of the circular, negative features identified from the MOLA shaded relief map. The number beside each MOLA track corresponds to the crater reference number in Table 1 and the presented tracks are organized by depth. The number of tracks used for validation of each impact crater is also listed in Table 1.

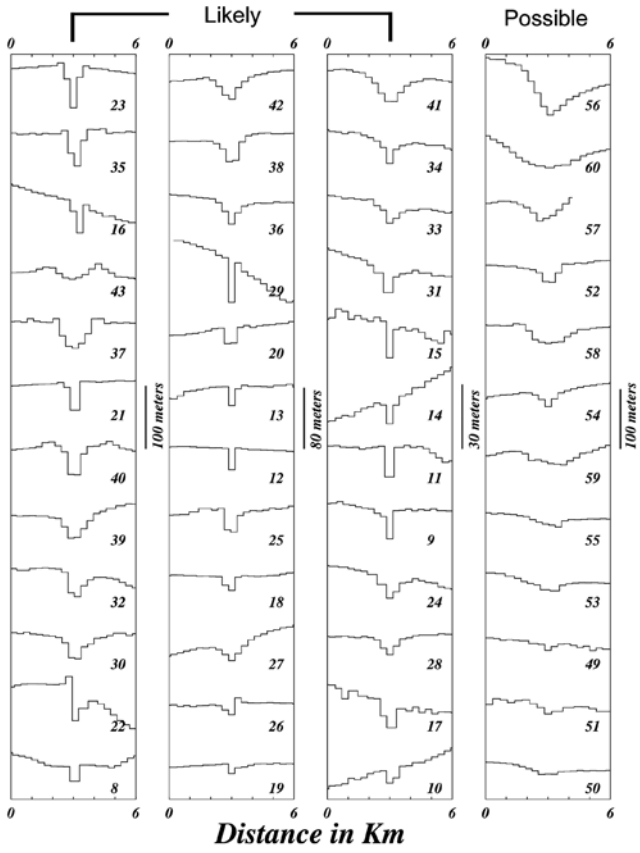

Figure 2. Selected MOLA tracks for each of the 36 likely and the 12 possible SPLD impact craters from 0.8 to 5 km in diameter. The first three columns are the 36 likely impact craters and the last column contains the 12 possible craters. The plots show the MOLA track at the different scales indicated to the right of each section and the along track distance is given in km. There are approximately 20 MOLA footprints in each 6 km profile. The number next to each plot corresponds to the impact crater identification number from Table 1.

[10] Nearly 500 MOC WA images through MGS mapping phase 18 in the sample study area were also surveyed for craters. These MOC WA images did not show many of the craters identified from the MOLA shaded relief map. Only 5 circular, negative features could be confidently identified as impact craters and 4 features identified as possible impact craters from the MOC WA images. There were another 7 MOC WA images that possibly show a crater identified from the MOLA shaded relief map but in these images the crater was more difficult to distinguish. The MOC WA images have a nadir resolution of approximately 250 m/pixel, making them most comparable to the Viking imagery. The number of craters visible in the MOC WA and the number of craters visible in the previous search using Viking imagery [*Plaut et al.*, 1988] is shown to be very limited compared to the population of SPLD impact craters identified in this study.

[11] Approximately 1400 MOC NA images through mapping phase 18 in the sample study area were also searched for impact craters. The MOC NA images are high-resolution (down to 1.5 m/pixel) and cover approximately 7.2×10^4 km^2 of the SPLD, only about 15% of the total sample study area. This value was derived using GIS and accounts for MOC NA image overlap. The MOC NA used in this study have a resolution range of 1.5–12 m/pixel. The coverage area of the MOC NA is most complete near 87°S to approximately 85°S and is much less complete over the area where most of the MOLA validated impact crater population has been identified. This resulted in only 2 images from this MOC NA search that went over craters that we previously identified on the MOLA shaded relief map. Figures 3a and 3b show the only MOC NA images we found that happen to cover any of the MOLA validated SPLD likely craters. These two craters seen in the MOC NA show very little evidence for a raised rim and are shallow (approximately 45 m deep), as can be seen in the associated MOLA tracks.

[12] However, the detailed survey of MOC NA images also resulted in recognition of a limited population of impact craters smaller than 800 m that could not be seen on the MOLA shaded relief map because they were below the limit of resolution of the map. There is also a "likely" and "possible" classification for this small impact crater population. The smaller than 800 m MOC NA likely craters are circular, negative, bowl-shaped features that do not show associations with and are not located near suspected secondary crater fields or endogenic features. The MOC NA possible craters are circular, negative features but could not be determined to have a most likely primary impact origin. There are a total of 8 likely impact craters less than 800 m, with a smallest crater diameter of approximately 20 m. We consider another 5 negative features as possible impact craters from MOC NA image analysis. The MOC NA images covering the 8 likely impact craters are shown in Figure 4 and the associated statistics are given in Table 2. The listing of all likely and possible craters and associated statistics are presented in Table 1.

2.2. Sample Area Determination

[13] A sample study area of the SPLD was carefully selected to reduce the counting of: (1) impact craters in subjacent, older units that may show through thin regions of SPLD, (2) obvious secondary impact crater swarms, and (3) possible crater-like endogenic features. This selected sample area is 5.2×10^5 km^2, approximately 40% of the entire exposed SPLD. In our judgment it is the area of the SPLD where the primary impact craters can be most unambiguously identified. This sample study area with the locations of the likely and possible impact craters is shown in Figure 1 along with the more inclusive boundary of the mapped SPLD [*Kolb and Tanaka*, 2001]. The portion of the mapped SPLD equatorward of approximately 80°S was excluded because there are some underlying impact craters whose outlines are reflected in the SPLD surface and there are also some probable secondary impact crater populations. The crater McMurdo (84.5°S, 0°W) and its surrounding secondary field were also excluded. The south polar residual cap was excluded because of the many circular, negative features noted to be of possible or likely endogenic origin when examined using the high-resolution MOC NA images that cover the portion of the residual cap mapped by MGS [*Thomas et al.*, 2000]. Finally, neither MOC nor MOLA

Table 1. SPLD Impact Craters

Number	Latitude	Longitude, W	Diameter, km	MOLA Tracks		Minimum		Image Coverage
				Points	Traces	Rim, m	Depth, m	
				Likely Impact Craters				
1	−85.8	329.6	0.02	–	–	–	–	MOC NA m09-06430
2	−85.0	308.4	0.03	–	–	–	–	MOC NA m09-00185
3	−82.6	45.5	0.12	–	–	–	20	MOC NA m10-01138
4	−86.5	132.3	0.14	–	–	–	–	MOC NA m03-04459
5	−86.5	118.2	0.27	–	–	–	–	MOC NA m10-02964
6	−80.7	260.0	0.37	–	–	–	70	MOC NA m09-01322
7[a]	−87.0	225.3	0.67	–	–	–	–	MOC NA m09-03768
8	−85.3	121.9	0.8	2	2	–	30	–
9	−81.9	172.3	0.8	2	7	2	10	–
10	−82.0	167.2	0.8	2	2	–	5	–
11	−83.8	118.2	0.9	2	6	–	10	–
12	−81.6	132.4	0.9	2	2	–	20	–
13	−83.5	273.0	1.0	3	3	2	20	–
14	−83.4	153.2	1.0	3	2	–	10	–
15	−85.2	239.8	1.0	3	8	5	10	–
16	−81.8	293.6	1.0	2	3	–	45	MOC NA m09-02042
17	−81.1	138.4	1.1	3	5	2	6	–
18	−83.4	132.7	1.1	2	2	–	15	possible MOC WA m07-05624
19	−82.1	170.9	1.2	4	2	4	11	–
20	−83.5	114.3	1.2	3	5	8	21	–
21	−83.7	148.6	1.3	4	5	6	35	–
22	−85.8	157.4	1.3	3	5	–	30	–
23[a]	−83.8	250.1	1.4	5	5	–	65	likely MOC WA m07-06024
24	−82.0	130.4	1.4	5	5	–	8	likely MOC WA m07-06024
25	−83.1	175.3	1.5	4	2	–	18	–
26	−82.7	181.4	1.5	5	4	6	12	–
27	−80.1	256.5	1.6	6	6	–	12	–
28	−81.1	121.1	1.6	5	6	–	7	–
29	−83.9	270.7	1.6	12	2	–	23	–
30	−83.5	270.7	1.6	5	9	–	30	–
31	−82.8	146.7	1.7	6	4	–	10	–
32	−83.8	275.9	1.7	6	5	–	30	–
33	−81.9	140.1	1.7	5	5	–	10	–
34	−83.2	144.7	1.8	5	5	–	10	likely MOC WA m07-05886
35	−86.2	150.2	1.9	5	25	5	45	MOC NA m03-04729
36	−81.9	142.2	2.1	7	8	–	25	likely MOC WA m07-01004
37[a]	−83.6	168.5	2.2	6	11	8	38	likely MOC WA m07-01040
38	−80.4	122.3	2.3	7	4	–	25	–
39	−85.6	131.9	2.6	8	18	8	30	possible MOC WA m07-03381
40	−82.3	157.8	2.6	10	6	10	30	likely MOC WA m07-05656
41	−83.8	147.5	2.7	10	5	–	10	possible MOC WA m07-02714
42	−80.0	254.0	2.8	8	8	–	25	likely MOC WA fsm07-04226
43[a]	−80.8	248.3	3.2	16	5	15	42	possible MOC WA m07-04802
				Possible Impact Craters				
44	−84.1	312.6	0.02	–	–	–	–	MOC NA m08-07864
45	−80.8	132.3	0.08	–	–	–	–	MOC NA m11-01528
46	−85.0	160.4	0.12	–	–	–	–	MOC NA m08-03912
47	−81.0	239.8	0.16	–	–	–	–	MOC NA m08-06243
48	−79.8	111.9	0.17	–	–	–	–	MOC NA m07-04185
49	−83.2	186.4	1.3	5	2	–	10	–
50	−81.8	157.0	1.8	4	3	–	5	likely MOC WA m07-05656
51	−82.5	122.7	1.8	5	5	–	9	–
52	−80.2	158.9	1.9	7	2	–	27	–
53	−82.3	164.7	2.1	9	8	–	10	possible MOC WA m07-05656
54	−80.8	127.8	2.3	6	8	2	20	possible MOC WA m07-03600
55	−82.8	160.4	2.7	9	14	–	10	possible MOC WA m07-05656
56	−82.9	276.4	2.8	9	12	–	45	–
57	−83.9	125.0	2.9	10	10	2	28	–
58	−82.4	167.0	3.0	10	11	3	25	likely MOC WA m07-00601
59	−82.3	165.5	3.2	9	12	6	15	likely MOC WA m07-00601
60	−81.7	154.6	4.7	17	15	–	40	likely MOC WA m07-05002

[a] = identified by *Plaut et al.* [1988].

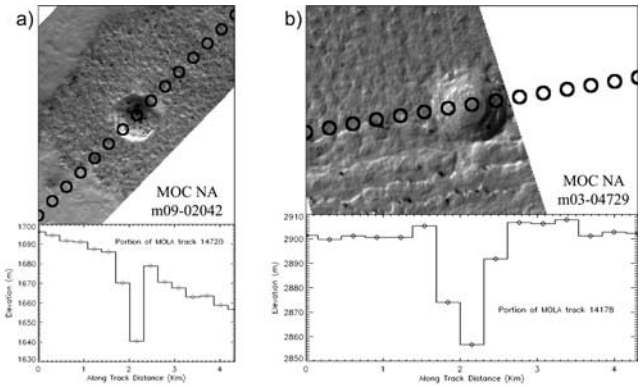

Figure 3. (a) A portion of MOC NA frame m03-04729 at 86°S, 150°W and MOLA track 14720 showing the impact crater identified by number 35 in Table 1. (b) A portion of MOC NA frame m09-02042 at 82°S, 293°W and MOLA track 14178 showing the impact crater identified by number 16 in Table 1.

data sets are complete between 87°S–90°S latitude, so this entire area was also excluded.

2.3. Validation Methods

[14] All of the features originally identified on the MOLA shaded relief map had to satisfy the following criteria in order to be validated here as "likely" impact craters: (1) roughly circular on the MOLA shaded relief map, (2) topographically negative, (3) consistent with a bowl-shaped or filled bowl-shaped from individual MOLA tracks, and (4) located in the selected sample study area of the SPLD. Any evidence of a raised rim and/or ejecta blanket from analysis of MOLA profiles provided further support for a likely classification. The outlined criteria could not be satisfied from the MOLA shaded relief map identification alone. Hence, the individual MOLA tracks were required unless a MOC NA frame resolved the suspect feature. Any feature that was negative but was not adequately circular or bowl-shaped was considered a "possible" impact crater. We expect that using future higher-resolution data these features generally will be interpreted as degraded impact structures.

[15] In the absence of complete MOC NA coverage, the best method of impact crater validation proved to be obtaining the individual MOLA tracks located in close proximity to the circular, negative features identified from the MOLA shaded relief map. From this it became apparent whether the feature displayed a characteristic impact crater profile in the MOLA track or was an obvious aberration of the shaded relief map. The MOLA shaded relief map aberrations generally are the result of a single false negative MOLA pixel in a single MOLA track that propagated into a false circular, negative feature a few pixels across on the shaded relief map when the MOLA data were gridded to the continuous map surface. The crossing tracks for all circular, negative features identified from the MOLA shaded relief map were checked to distinguish which features were aberrations and which were real impact craters. All impact craters comprising the likely population and the possible population over 800 m in diameter have more than one crossing MOLA track that confirms that they are real negative surface features, not single point aberrations.

3. Data Analysis

3.1. SPLD Crater Population

[16] Table 1 presents the numerical results for all the likely and possible impact craters in the study area. The crater diameter listed is rounded to the nearest hundred meters from the diameter obtained from the MOLA shaded relief map and, if applicable, the MOLA tracks that crossed near the center of the crater or MOC NA images. The MOLA shaded relief map was used for diameter measurements because it incorporates all the data and is higher resolution than a single MOLA track crossing the impact crater. Table 1 also provides the number of MOLA tracks that cross the impact crater, the maximum number of MOLA pixels wide each crater is observed to be, the measured rim height, and the measured crater depth.

[17] The sample study area is 5.2×10^5 km^2 and all data plotted were in the 0.8–5 km diameter range. There are 36 likely impact craters and 12 possible impact craters in this range. This search has resulted in identification of at least four times the density of impact craters on the SPLD than previously recognized [*Plaut et al.*, 1988]. Of these craters, the craters with reference number 23 and 37, as listed in Table 1, are the only craters in the sample area identified by *Plaut et al.* [1988] as likely using Viking imagery. These were also independently found in this work as part of our likely population. There are four other features in our study area identified by *Plaut et al.* [1988] as possible impact

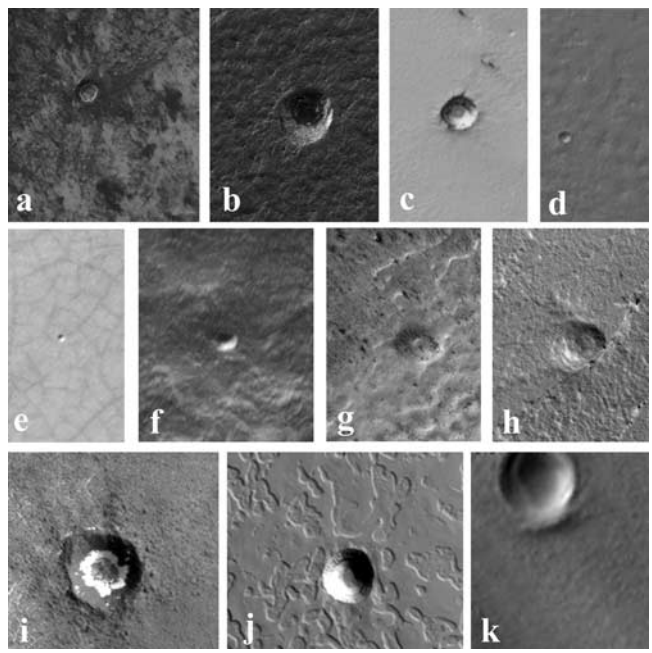

Figure 4. Figures a to h show the MOC NA images for all the likely impact craters smaller than 800 m. Figure i is off the SPLD, j is on the south residual cap, and k is on the NPLD and all are shown for comparison to the impact craters on the SPLD. All the images are at different scales. Table 2 gives complete information for these craters.

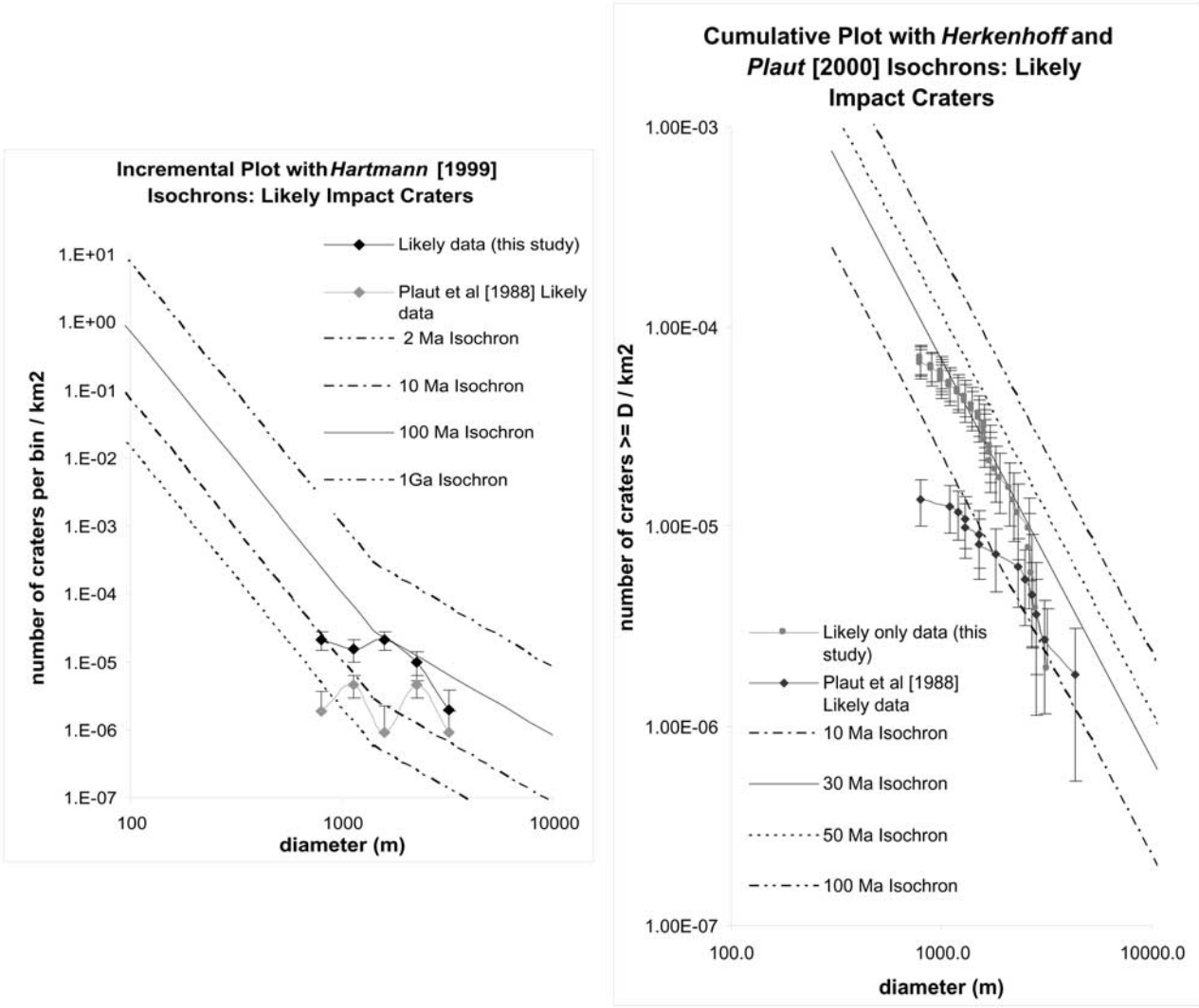

Figure 5. (a) The likely SPLD impact crater population for crater diameters 0.8 to 5 km and the *Plaut et al.* [1988] likely SPLD crater population compared to the *Hartmann* [1999] production model isochrons, in incremental format. The SPLD likely data gives an estimated mean apparent surface age of 90 Ma. (b)The likely SPLD impact crater population for crater diameters 0.8 to 5 km and the *Plaut et al.* [1988] likely SPLD crater population compared to the *Herkenhoff and Plaut* [2000] production model isochrons, in cumulative format. The SPLD likely data gives an estimated mean apparent surface age of 30 Ma.

craters. We have classified two of these possible craters as likely by finding them in a MOC NA image or individual MOLA tracks. They are identified by reference number 7 (see also Figure 4g) and by reference number 43. One of the other two *Plaut et al.* [1988] possible crater locations is in close proximity to a crater observed in this study, but the other one is not near anything we were able to validate. We did not include either of these two possible impact craters because they did not satisfy our validation criteria.

[18] *Hartmann* [1999] has developed a general crater population dating system that involves plotting isochrons in conjunction with incremental (as opposed to cumulative) crater size-frequency data. A *Hartmann* [1999] isochron is an expected incremental size-frequency distribution for a surface of a given age. The *Hartmann* [1999] isochron shape has a ''primary branch'' and a ''secondary branch'' to represent the complex structure of the crater production function. The primary branch has a slope of -1.80 and the secondary branch has a slope of -3.82 with a turndown slope of -2.2 at $D > 64$ km [*Hartmann*, 1999]. Surface ages determined from the isochrons assume the effects of deposition and erosion are negligible [*Hartmann*, 1999]. This results in a mean apparent age that is likely younger than the true surface age if erosion and deposition were considered.

[19] In the interest of comparing our data with the previous study done by *Herkenhoff and Plaut* [2000] we have utilized their cumulative isochrons. In the *Herkenhoff and Plaut* [2000] production model that is specific to the PLD, different from *Hartmann* [1999], a cumulative crater size frequency power law with slope of -2 was used to extrapolate the ''nominal'' R(20) value of 5.6 (twice the lunar value) or the ''high'' R(20) of 11.2 (four times the lunar value) to smaller diameters [*Herkenhoff and Plaut*, 2000]. The production model isochrons from *Herkenhoff*

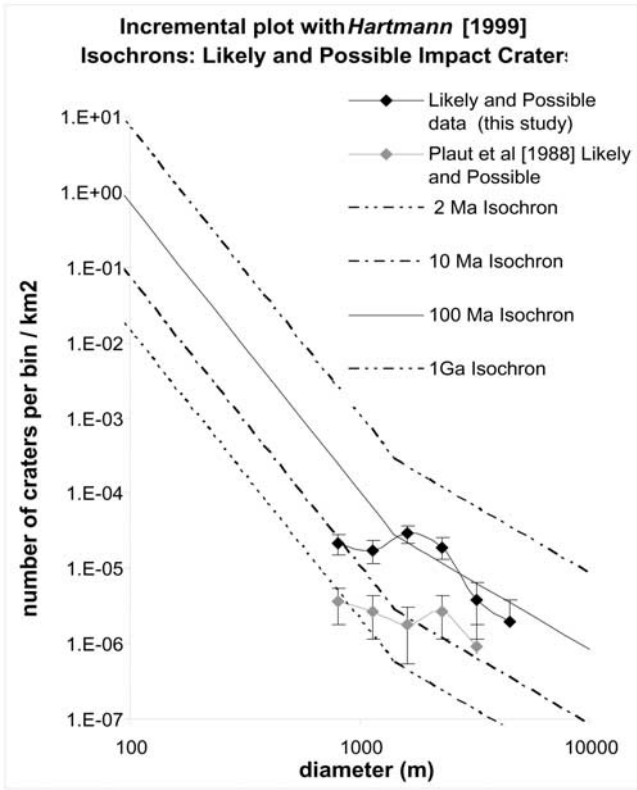

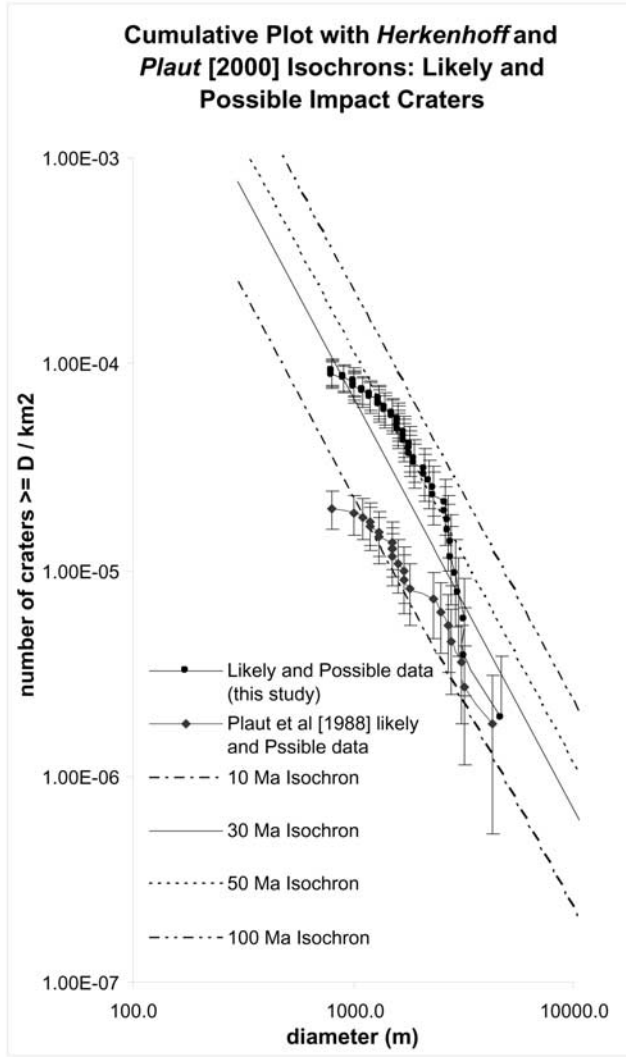

Figure 6. (a) The combined likely and possible SPLD impact crater population for crater diameters 0.8 to 5 km and the *Plaut et al.* [1988] likely and possible SPLD crater population compared to the *Hartmann* [1999] production model isochrons, in incremental format. The combined SPLD likely and possible data give an estimated mean apparent surface age of 100 Ma. (b) The combined likely and possible SPLD impact crater population for crater diameters 0.8 to 5 km and the *Plaut et al.* [1988] likely and possible SPLD crater population compared to the *Herkenhoff and Plaut* [2000] production model isochrons, in cumulative format. The combined SPLD likely and possible data give an estimated mean apparent surface age of 50 Ma.

and Plaut [2000] correspond only to their nominal cratering rate of R(20) = 5.6. *Hartmann et al.* [1981] believes that twice the lunar value, R(20) = 5.6, is the "most likely" value and is why this was used primarily by *Herkenhoff and Plaut* [2000]. In the *Herkenhoff and Plaut* [2000] model, crater obliteration is accounted for as a constant vertical resurfacing process that removes craters in a way that is depth-dependent. We have not developed an independent cratering model for the PLD. We compare our data to the *Hartmann* [1999] and the *Herkenhoff and Plaut* [2000] production models.

[20] These two different production models were plotted in comparison to both the likely only population and the likely and possible populations from this study and from the *Plaut et al.* [1988] study. The differences in the models, as outlined above, account for the differences in the resultant model surface ages that are presented here. In comparison to both the *Hartmann* [1999] and the *Herkenhoff and Plaut* [2000] model isochrons our data did not fit a particular isochron exactly for the entire diameter range. When assigning a surface age from the two different models we chose the isochron that our data most followed for the larger (over 2 km) craters. This is the part of the population that most resembles a production population and is consistent with the method used by *Herkenhoff and Plaut* [2000].

[21] The likely SPLD crater population is compared to the likely *Plaut et al.* [1988] crater population in Figure 5. The log-incremental plot in Figure 5a shows that all the likely data from this study result in a mean apparent surface age of approximately 80 Ma according to the *Hartmann* [1999]

isochrons. Figure 5b is the cumulative representation of both data sets in comparison to the *Herkenhoff and Plaut* [2000] isochrons and results in an age estimate of approximately 30 Ma. The combined likely and possible validated SPLD crater population compared to the likely and possible *Plaut et al.* [1988] crater population is shown in Figure 6. We judge the combined likely and possible crater population from this study to be a better estimate of the entire impact crater population than the likely data alone. According to the *Hartmann* [1999] isochrons, as shown in Figure 6a, the age of the SPLD using this entire population of likely and possible validated craters is approximately 100 Ma. The mean apparent surface age of the SPLD surface using the *Herkenhoff and Plaut* [2000] production model, as shown in Figure 6b, is approximately 50 Ma. The difference in these age estimates is due to the differences in the two production models we compare.

[22] The data from this study fit the *Herkenhoff and Plaut* [2000] model isochrons in the approximately 1–2 km diameter range. In comparison, only a small section of the *Plaut et al.* [1988] data trends toward a particular model isochron. This is due to the inability to identify small impact craters and especially shallow impact craters from the data sets available previous to the MGS mission. There are only a few larger diameter craters in the sample study area that could be identified because of the limited size of the study area. The observed fall-off from the isochron in both production models at the largest diameters is due to these low statistics. The fall-off at approximately 0.8–1.2 km from the *Hartmann* [1999] isochron is possibly due to low statistics in that size bin because of the resolution limit of the MOLA data and the lack of coinciding MOC NA coverage.

[23] As a check on the reliability of the statistical significance of this analysis a randomly generated crater production population was created and this was compared to the crater population in this study. We assumed that the cumulative probability distribution follows a power law and used a random number generator with uniform distribution between 0 and 1. A simulation was done to model a crater population in the diameter range of 0.8–5 km using a random number generator and solving for the radius of each simulated impact. The calculated diameters were then plotted with the actual crater population from this study in comparison to the *Herkenhoff and Plaut* [2000] model isochrons. In multiple trials the simulated data were always within the error bars of the actual data and had the same nonlinear, disjointed line style as seen for the actual data in Figures 5b and 6b. This supports the reliability of the production model isochrons with the number of craters included in this population.

3.2. South Polar Residual Cap Data and North Polar Data

[24] We also searched the south polar residual cap, which was not included in our study area, for impact craters using the same techniques described above. The outline of the residual cap has been approximately mapped using MOC WA image M14-01236 (Ls = 337.04°). The portion of the MOLA shaded relief map covering the outlined south polar residual cap does not show the same distribution of circular, negative features as the rest of the SPLD. Using the validation techniques described above, no craters in the 800 m and larger range from the MOLA shaded relief map could be validated by individual MOLA tracks on that portion of the residual cap equatorward 87°S. Out of all circular, negative features identified from the survey of 370+ MOC NA images only one could be identified as a probable impact crater (e.g., M09-06496). This impact crater has been previously identified by *Herkenhoff* [2001] in an aerobraking image and has a diameter of approximately 215 m, a depth of approximately 40 m, and is shown in Figure 4j. Except for this one crater, the lack of craters on the south polar residual cap is also consistent with the observation by *Thomas et al.* [2000] that there are no obvious impact craters with diameters greater than 100 m in the more than 550+ MOC NA images they surveyed of the south polar residual cap. Recently presented by *Malin et al.* [2001], changes have been seen in features on the south residual cap that indicate it is an active surface that could have an effect on the impact crater population there.

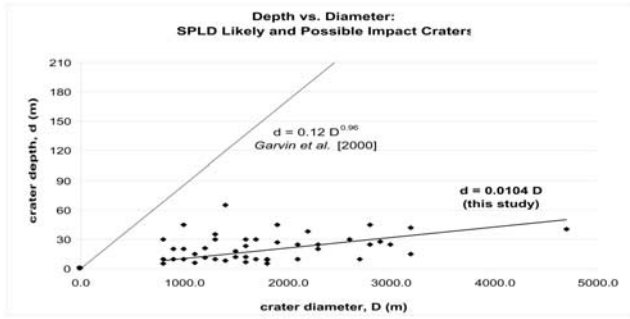

Figure 7. Depth versus diameter for all likely and possible impact craters in our study area of the SPLD with diameters from 0.8 to 5 km. All the craters in this population are very shallow in comparison to the trend line using the depth to diameter relation of $d = 0.12\ D^{0.96}$ from *Garvin et al.* [2000] for midlatitude craters less than 7 km in diameter.

[25] The North Polar Layered Deposits (NPLD) have been reported to be completely devoid of impact craters (larger than 300 m in diameter) based on analysis of Mariner 9 and Viking data [*Cutts et al.*, 1976; *Herkenhoff and Plaut*, 2000]. Thus far we have been able to identify only one crater in a MOC NA image (M01-02447). This crater is approximately 300 m in diameter and is shown in Figure 4k. *Malin and Edgett* [2001] also report finding an impact crater in MOC NA M19-01628 and we have confirmed it with 46 m in diameter. We have not done a complete survey of all MOC NA images of the NPLD, but a search for craters using the north polar MOLA shaded relief map was completed. Applying the same criteria used for the SPLD no impact craters approximately 800 m or larger in diameter could be observed or validated on the NPLD. This lack of craters is consistent with previous Viking orbiter data [*Herkenhoff and Plaut*, 2000] and may not likely be a surprising result because the NPLD is mostly covered by the residual cap.

3.3. SPLD Crater Characteristics

[26] The individual MOLA tracks associated with each validated impact crater provide information about crater depth, diameter, and rim height, if prominent. The profile showing maximum relief was chosen for each crater, as

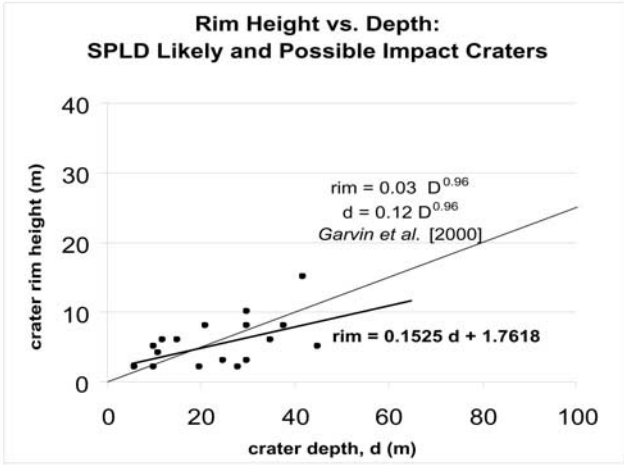

Figure 8. Crater depth versus crater rim height for all likely and possible impact craters validated on the SPLD with diameters from 0.8 to 5 km for which a rim could be calculated. Our data is compared to the rim height relationship from *Garvin et al.* [2000] for midlatitude craters less than 7 km in diameter. The retention of crater rims while the craters are unusually shallow suggests that there cannot only be a process of deposition. We suggest that there is one process that is eroding away the rims and one process that is infilling the craters.

shown in Figure 2. The depth and rim height for that crater was measured from that track. The complete list of the measurements associated with each of the validated craters is presented in Table 1.

[27] Our most significant finding in regards to crater morphology is that the SPLD craters are generally much shallower than their counterparts elsewhere on Mars. We note that the MOLA tracks may not cross the center of the crater and could result in a shallower measured depth, though even considering this effect the population of impact craters on the SPLD is very shallow. The plot of depth compared to diameter for all the SPLD likely and possible impact craters is shown in Figure 7. These data are compared to the depth to diameter trend line for midlatitude Martian craters that are less than 7 km in diameter using the relation $d = 0.12\ D^{0.96}$ (where d = depth and D = diameter) given by *Garvin et al.* [2000], determined using MOLA data. Our trend line shows a slight positive correlation between crater diameter and depth, but all the craters are shown to be extremely shallow in comparison to the depths expected for other Martian craters in that same diameter range. There does not appear to be an obvious correlation between the crater depths and crater locations on the sample study area of the SPLD. Therefore crater depth may be mostly a function of crater age.

[28] Crater depth does correlate with crater rim height, as evident in Figure 8, which plots depth versus rim height for all likely and possible craters for which a rim could be detected from MOLA profiles. Our data has been compared to the rim height to crater diameter trend line for other Martian midlatitude craters that are less than 7 km using the relation $rim = 0.03\ D^{0.96}$ (D = diameter) and the depth to diameter relation $d = 0.12\ D^{0.96}$ (where d = depth and D = diameter) given by *Garvin et al.* [2000], determined using MOLA data. This shows that there is retention of crater rims even with a shallow crater depth and therefore the process of crater infill cannot be due to blanketing alone.

4. Discussion and Conclusions

[29] The previous lower estimate of impact craters on the SPLD compared to this MOLA/MOC study can be primarily attributed to the inability to recognize the unusually shallow SPLD impact craters in Mariner 9 and Viking visible imagery. This new crater population implies a mean apparent surface age for the SPLD of approximately 30–100 Ma, based on production model isochrons from *Herkenhoff and Plaut* [2000] and *Hartmann* [1999]. It is evident from Figure 1 that the abundance of validated impact craters on the sample study area of the SPLD clusters around 90°W–180°W. It is possible that this area is a more stable, older exposure of SPLD. In addition, nearly all of the possible impact craters also are in this region, which could indicate that they are in fact older, degraded impact craters as we have speculated earlier in this paper.

[30] The apparent surface age estimate of 30–100 Ma is greater than the previous estimate of approximately 10 Ma [*Plaut et al.*, 1988; *Herkenhoff and Plaut*, 2000]. The timescales postulated for layer formation driven solely by deterministic climatic fluctuations of about 10^5–10^6 years [*Ward*, 1974] or possible chaotic fluctuations of up to 10^7 years [*Touma and Wisdom*, 1993] cannot explain why south polar layered deposition would have ceased 30–100 Ma. Thus the surface of the SPLD included in our study may record some event in polar history that marked the end of layer formation at least in that area.

[31] Morphologically, the SPLD impact craters are all anomalously shallow, as indicated in Figure 7. We suggest that a local process of crater infill must have occurred.

Table 2. Less Than 800 m SPLD Impact Craters

Crater	Diameter, m	Depth, m	MOC NA	Ls	Comments
a	270	–	m10-02964	270.28°	possible evidence of ejecta
b	370	70	m09-01322	238.46°	–
c	120	20	m10-01138	260.48°	slight raised rim
d	140	–	m03-04459	175.40°	–
e	20	–	m09-06430	252.97°	smallest observed on SPLD
f	30	–	m09-00185	235.99°	–
g	670	–	m09-03768	244.41°	identified by *Plaut et al.* [1988]
h	550	–	m03-04947	176.68°	–
i	200	30	m10-03666	273.61°	off the SPLD
j	215	40	m09-06496	253.12°	on the south residual cap
k	330	30	m01-02447	140.72°	on the NPLD

However, 30% of the impact craters also exhibit raised rims that could be determined from the crossing MOLA tracks available, as shown in Figure 8. Blanketing alone cannot explain both the amount of crater infill and the retention of some rims. A new model for crater resurfacing is required by these observations involving at least one process of erosion that is removing the rims and a second process to account for the strong infilling of the craters. A model of viscous creep relaxation of a dusty water ice surface has been shown to have a significant shallowing of crater depth over time while having minimal effect on crater rims [*Pathare et al.*, 2002].

[32] In addition, there is yet another clue to the history of this surface. The observed SPLD impact craters with diameters smaller than 800 m exhibit quite different characteristics than do the rest of the SPLD crater population presented in this work. First of all, the craters with diameters smaller than 800 m that could be identified in MOC NA are very rare. We found only 8 likely and another 6 possible impact craters in the diameter range of 20 m–700 m in the portion of our study area with MOC NA coverage. However, it is noted that the crater distribution within our study area is not uniform, as exhibited in Figure 1. While the MOLA data uniformly covers the study area the MOC NA data primarily cover an area with a lower large crater abundance. When the MOC NA crater data are normalized to the 7.2×10^4 km^2 area of MOC NA coverage, and compared to the *Hartmann* [1999] isochrons, the crater retention age for this diameter range can be estimated at approximately 100,000 years. Alternatively, the *Hartmann* [1999] production model isochron for a mean apparent surface age of 100 Ma (which fits the 0.8–5 km combined likely and possible crater population) shows there should be at least 300,000 craters observed over the area covered with MOC NA images in our study area with diameters 100 m–700 m assuming no resurfacing. This number of craters is at least three orders of magnitude more than we actually found. Hence, the number of small impact craters observed shows that there has been significant removal of 100–700 m craters on the SPLD compared to those craters over 800 m in diameter. In addition, we have also found that these smaller craters are proportionately deeper than the 0.8–5 km diameter craters. From shadow measurements the depths of a few of the smaller craters were estimated and are listed in Table 2.

[33] The observation that the smaller craters are rare and that the larger craters are more abundant and very shallow could suggest that there may have been an episode of resurfacing in the recent past that removed all the smaller craters but left the larger ones shallow but recognizable.

[34] Greater coverage of high resolution imagery data over the SPLD, especially from the Odyssey spacecraft visible THEMIS instrument, will provide further validation of the impact craters identified in this study and probably reveal many other small impact craters unable to be identified. We will extend these analyses to the rest of the SPLD and to the NPLD. It will be important to model carefully the morphologies of the craters, especially to distinguish, if possible, between depositional or deformational effects acting on the impact crater population of the SPLD.

[35] **Acknowledgments.** We thank Ken Herkenhoff (USGS) and Jeff Plaut (JPL) especially for their continual review of this work. Acknowledgment is given to the MOC and MOLA science teams, Ken Tanaka and Eric Kolb (USGS) for providing an updated mapped outline of the SPLD, and to Anton Ivanov (JPL/Caltech) for providing a MOLA data search tool. Thanks to Zane Crawford and Peter Marsden for their assistance in searching MOC images. This paper has also greatly benefited from reviews and criticism by Asmin Pathare (UCLA), Andrew Ingersoll (Caltech), and Arden Albee (Caltech).

References

Albee, A. L., R. E. Arvidson, F. Palluconi, and T. Thorpe, Overview of the Mars Global Surveyor mission, *J. Geophys. Res.*, *106*, 23,291–23,316, 2001.

Cutts, J. A., K. R. Blasius, G. A. Briggs, M. H. Carr, R. Greeley, and H. Masursky, North polar region of Mars: Imaging results from Viking 2, *Science*, *194*, 1329–1337, 1976.

Garvin, J. B., S. E. H. Sakimoto, C. Schnetzler, and J. J. Frawley, Global geometric properties of Martian impact craters: A preliminary assessment using Mars Orbiter Laser Altimeter (MOLA), presented at the Lunar and Planetary Science Conference (LPSC) XXXI, Houston, Texas, 2000.

Hartmann, W. K., Martian cratering, 6, Crater count isochrons and evidence for recent volcanism from Mars Global Surveyor, *Meteorit. Planet. Sci.*, *34*, 167–177, 1999.

Hartmann, W. K., et al., Chronology of planetary volcanism by comparative studies of planetary cratering, in *Basaltic Volcanism on the Terrestrial Planets*, Basaltic Volcanism Project, pp. 1049–1127, Pergamon, New York, 1981.

Herkenhoff, K. E., Geologic map of the MTM—85000 Quadrangle, Planum Australe Region of Mars, *U.S. Geol. Surv. Misc. Invest. Ser. Map*, *I-2686*, 2001.

Herkenhoff, K. E., and J. J. Plaut, Surface ages and resurfacing rates of the Polar Layered Deposits on Mars, *Icarus*, *144*, 243–253, 2000.

Howard, A. D., J. A. Cutts, and K. R. Blasius, Stratigraphic relationships within Martian Polar Cap Deposits, *Icarus*, *50*, 161–215, 1982.

Kahn, R., The spatial and seasonal distribution of Martian clouds, and some meteorological implications, *J. Geophys. Res*, *89*, 6671–6688, 1984.

Kolb, E., and K. Tanaka, presented at the Lunar and Planetary Science Conference (LPSC) XXXII, Houston, Texas, 2001.

Malin, M. C., and K. S. Edgett, The Mars Global Surveyor Mars Orbiter Camera: Interplanetary cruise through primary mission, *J. Geophys. Res.*, *106*, 23,429–23,570, 2001.

Malin, M. C., M. A. Caplinger, and S. D. Davis, Observational evidence for an active surface reservoir of solid carbon dioxide on Mars, *Science*, *294*, 2146–2148, 2001.

Murray, B. C., L. A. Soderblom, J. A. Cutts, R. P. Sharp, D. J. Milton, and R. B. Leighton, Geological framework of the South Polar Region of Mars, *Icarus*, *17*, 328–345, 1972.

Neumann, G. A., D. D. Rowlands, F. G. Lemoine, D. E. Smith, and M. T. Zuber, The crossover analysis of MOLA altimetric data, *J. Geophys. Res.*, *106*, 23,753–23,768, 2001.

Pathare, A. V., D. A. Paige, E. P. Turtle, and W. K. Hartmann, Viscous creep relaxation of impact craters within the Martian Polar Layered Deposits, presented at the Lunar and Planetary Science Conference XXXIII, 2002.

Plaut, J. J., R. Kahn, E. A. Guiness, and R. E. Arvidson, Accumulation of sedimentary debris in the South Polar Region of Mars and implications for climate history, *Icarus*, *75*, 357–377, 1988.

Thomas, P., S. Squyres, K. Herkenhoff, A. Howard, and B. Murray, Polar deposits of Mars, in *Mars*, edited by H. H. Kieffer, B. M. Jakosky, C. W. Snyder, and M. S. Matthews, pp. 767–795, Univ. of Ariz. Press, Tucson, 1992.

Thomas, P. C., M. C. Malin, K. S. Edgett, M. H. Carr, W. K. Hartmann, A. P. Ingersoll, P. B. James, L. A. Soderblom, J. Veverka, and R. Sullivan, North–south geological differences between the residual polar caps on Mars, *Nature*, *404*, 161–163, 2000.

Touma, J., and J. Wisdom, The chaotic obliquity of Mars, *Science*, *259*, 1294–1297, 1993.

Ward, W. R., Climatic variations on Mars, 1, Astronomical theory of insolation, *J. Geophys. Res.*, *79*, 3375–3386, 1974.

Zuber, M. T., D. E. Smith, S. C. Solomon, D. O. Muhleman, J. W. Head, J. B. Garvin, J. B. Abshire, and J. L. Bufton, The Mars Observer Laser Altimeter investigation, *J. Geophys. Res.*, *97*, 7781–7798, 1992.

S. Bryne, M. Koutnik, and B. Murray, Geological and Planetary Science, California Institute of Technology, MC 170-25, 1200 East California Boulevard, Pasadena, CA 91125, USA. (mkoutnik@gps.caltech.edu)